

Using Strain Gauges to Detect Epoxy Debonding in Insulated Rail Joints

Daniel Peltier, Christopher P. L. Barkan, Steven Downing, and Darrell Socie
University of Illinois at Urbana-Champaign, Urbana, IL, USA

Summary: Track circuits are used for traffic control on a large portion of North American mainline track. These require insulated rail joints every several kilometers in order to electrically isolate sections of the rail. Such insulated joints have short service lives compared to other track components, but current methods for monitoring their condition and detecting defects are either too involved for everyday use or insufficiently accurate. We are researching a new system based on low-cost smart sensor technology that will enable railroads to monitor the condition of insulated joints, plan for their maintenance or replacement, respond faster to problems, and collect statistical data about their performance. The system uses strain gauges to track the mechanical characteristics of a joint over time. By understanding how these properties change as the joint degrades, we can detect and report problems in a timely manner.

Index Terms: track structure, condition monitoring, sensor technology, system reliability

1. INTRODUCTION

Insulated rail joints are widely used throughout the North American rail network, occurring roughly every 5 km (3 miles) on almost all signaled track. These joints have shorter service lives than most other track components. Fortunately, most failures are not safety problems in and of themselves. But the magnitude of the problem, and the difficulty of obtaining good information about joint condition, makes keeping up with the necessary replacement work a challenge. The result is that insulated joint failure is more disruptive to railroad operations than it would be if failure could be detected automatically in time to schedule joint replacement in a rational manner. This paper focuses on the development of a technique and a technology for moni-

toring insulated joints that costs very little in terms of money, labor, or attention from the user.

2. INSULATED RAIL JOINTS

On North American heavy-haul railways, train control usually relies on various kinds of direct current (DC) track circuits to detect the presence of a train within a control block. Adjacent circuits within the track are separated by *insulated rail joints* (also called simply *insulated joints* or *IJ's*), a point where two separate rail sections are held together but electrically insulated from each other. Although these joints are always installed in pairs, one directly across from the other, most circuits will operate properly when separated by a single functioning joint, so long as the electrical resistance within that joint is sufficiently high. If both insulated

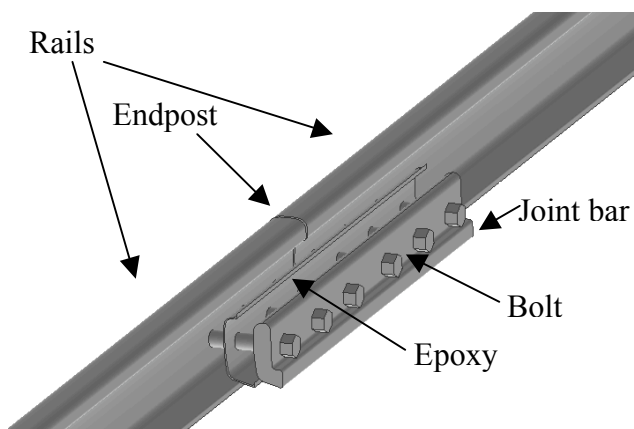
joints fail, the train control logic switches into a failsafe mode, displaying stop indications for all traffic through the area and disrupting operations.

2.2 Bonded insulated joint design

As with any rail joint, an insulated joint is a weak spot in the track structure. While the number of joints in mainline track has been minimized by the widespread use of continuously welded rail (CWR), North American railroads have not identified an acceptable alternative to track circuits with insulated joints. They have, however, migrated toward the use of *bonded insulated joints*. A bonded IJ, instead of being held together by bolts, has a layer of epoxy to bond the joint bars directly to the rails. The epoxy itself serves as the electrical insulator between the joint bars and the rails. Studies have shown that a bonded IJ is significantly stiffer (more like the welded rail surrounding it) than traditional bolted designs [1].

Figure 1 shows an exploded view of a typical bonded insulated joint, including the epoxy layer. While the assembly does have bolts, they do not have a significant effect on the action of the joint under loads. They mainly serve to provide a clamping force while the epoxy cures; after that, they act as a backup system in the event the epoxy fails. Thin insulating sleeves isolate the bolts from the web of the rail. Similarly, a fiberglass insert called an *endpost* ensures physical and electrical separation between the ends of the two rails, but is not designed to carry loads. Joint bar length, hole spac-

Figure 1: Exploded view of a bonded insulated joint



ing, and endpost thickness are more or less standardized. The thickness of the epoxy layers and the cross section of the joint bar vary from manufacturer to manufacturer.

With recent increases in North American axle loadings and annual tonnage, service lives of bonded IJ's have dropped substantially. Because of this, and because of improved designs and practices for other problematic track components, IJ's now have the shortest service life of any common track component in North American heavy-haul service, with the exception of high-angle rail crossings [2].

2.2 Insulated rail joint failure and inspection

Davis et al [2] describe the most typical failure of bonded insulated joints. Failure begins when the epoxy either cracks or comes unbonded from the metal surfaces of the rail at the point of maximum shear stress, which occurs near the endpost. As the bonding fails, the deflection of the joint under passing wheel loads increases. This leads to higher dynamic loads on the support system and higher differential movement between the rails and the bars, which in turn increases epoxy stress and hastens the debonding. The debonded region propagates back towards the ends of the joint bar. In this failure mode, a joint will usually be considered "failed" when the debonded region grows to an unacceptable level. Other problems that develop in a loose joint, such as broken bolts or loss of electrical resistance, may also lead to service failure.

There is no generally accepted standard for what constitutes an unacceptable amount of debonding, which may be due to the fact that there are no published studies quantifying the effect of epoxy damage on serviceability.

Aside from normal rail defect and geometry inspections, insulated joint inspection techniques fall into two categories: visual and electrical. Problems detectable by visual inspection include joint bar cracks, broken bolts, plastic flow of the rail head at the end post, and problems with crossties, fasteners, or longitudinal restraint. The inspector can also

examine the upper and lower edges of the epoxy layer (the only part of the layer visible to the eye) to detect the presence and estimate the size of a debonded region. Inspections are usually conducted on foot, due to the limited viewing angles available from a moving vehicle.

Starting January 1, 2007, the United States Federal Railroad Administration requires an on-foot visual inspection of certain components of insulated joints on most mainline freight railroads approximately once for every 18 million gross metric tons (20 million U.S. tons) of traffic [3]. These inspections are geared towards finding joint bar cracks, and do not require an assessment of epoxy condition.

Electrical inspections include various methods for testing the electrical resistance between one rail and the other. It can be difficult to perform these tests without interfering with the operation of the track circuit. Because electrical failures are designed to be fail-safe, electrical inspections of insulated joints tend to happen only when signal problems or visual inspections suggest a problem.

We believe that current insulated joint inspection practices are insufficient to ensure that the full service life is obtained while minimizing the likelihood of an operationally disruptive failure. The high number of insulated joint installations, the labor-intensive nature of available inspection techniques, and uncertainty about the extent and significance of epoxy loss even when a joint is inspected prevent maintenance personnel from scheduling insulated joint replacement in a timely but efficient manner.

3. SMART SENSORS

Wireless, self-networking sensors are becoming increasingly common in monitoring applications, keeping track of systems ranging from houses [4] to cattle [5]. The key behind such “smart sensors” is to package low-power microprocessors, short-range radios, and some sort of energy source along with a sensing element in a single integrated package. By including software to automatically detect

and network with other nearby sensors, a large number of sensors can be deployed in a given area with relatively little effort.

North American freight railroads have vast networks. They are therefore interested in technologies that can monitor their systems for problems without frequent human intervention. Such monitoring applications appear to be suitable applications for smart sensor technology.

Research at the University of Illinois at Urbana-Champaign has focused on developing smart sensors for engineering measurement applications. This effort has resulted in prototype “smart strain gauges”. These strain gauges require no bonding or soldering, and can perform their own data logging and processing. The use of low-cost, commodity parts wherever possible, and a focus on easy installation and minimal maintenance, makes these sensors usable for a number of structural and mechanical monitoring tasks that would not otherwise be economically feasible.

4. STRAIN RESPONSE MODELING

The application of smart sensor strain gauges to insulated joint monitoring first requires an understanding of what the measurable strains in a joint indicate about its condition. In other words, we must understand which strains to measure, and what values indicate failure.

4.1 Loadings considered

When designing an insulated joint, the most critical loading comes from wheels passing over the joint. The stresses that arise in the joint under wheel loads are the product of a complicated mix of factors, including train speed, wheel profile and defects, tie spacing, ballast fouling, and the presence of water or ice in the ballast or subgrade. Even for a single joint, these conditions can change over time. There is no obvious way to control for these variables using available smart sensors.

Fortunately, when designing a strain gauge-based insulated joint monitoring system, we need not focus on wheel loads. We are not interested so much in the maximum stresses or strains as we are in the strains that *change* as the joint deteriorates.

We propose that it is more productive to measure the strain of a joint in response to longitudinal thermal stresses. The main variables determining thermal stress are temperature, rail shape, joint design, and the longitudinal restraint offered by the fasteners and rail anchors.

Temperature varies widely throughout the day and throughout the year, but we can control for temperature change. Insulated joints are designed to handle wheel loads with little or no plastic deformation, so it is expected the behavior under thermally-induced loads will remain within the region of approximately linear response. If we look at the ratios of the thermally-induced strain at two or more different locations, and assume a linear-elastic response, the ratios stay constant regardless of the temperature change. Longitudinal restraint is expected to have only a small effect for a bonded joint [6, 7]. Thus we will focus on critical ratios of strains in response to thermal loads.

North American practice is to attempt to keep the neutral temperature of CWR high enough so that the rail is in tension more often than in compression. For this reason, we focus on the strain in the joint in response to thermal tensile forces; we assume that such forces will occur at least daily, allowing us to collect the measurements needed to detect deterioration.

4.2 Finite element model

A 3-dimensional solid finite element model was created to study the effects of thermal stresses on several insulated joint designs used in North America. The components included in the model were the two rails, the two joint bars, and the epoxy layer connecting joint bars to rails. Bolts were not included as they are not expected to carry any of the thermally-induced load.

The epoxy layer is composed of a single layer of elements. The outside surfaces are tied to the inner surfaces of the joint bar. The inner epoxy surfaces are connected to the rail via contact elements. The nature of these contact elements are altered to represent bonded surfaces, which transfer all loads, or debonded surfaces, which only transfer compression.

Two different geometries were used to model two common joint bar designs used in North America. Both joint bars are designed to fit rail either the 132RE or 136RE section, which weigh 67.5 kg/m (136 lb/yd) and 65.5 kg/m (132 lb/yd) respectively. The results below assume the heavier rail.

4.3 Finite element analysis

Figures 2 and 3 show the changes in strain on the outside surfaces of a fully-bonded insulated joint due to a decrease in rail temperature of 8.5°C (15.3°F). The two figures represent two different joint bar designs. The strains shown in the figures can be thought of as the superposition of two different actions: first, the natural compressive strain caused by the material contraction; and second, the tensile strains generated as free ends of the rails attempt to pull apart. For this temperature change, the unrestrained compression of steel would be approximately $-100\ \mu\epsilon$. This is the strain value at the ends of the joint bar.

An 8.5°C temperature change produces tensile loads of about 178 kN (40 kips) in fully restrained RE136 rails. This force must be resisted by the joint bars to prevent a pull-apart. The strains in the joint bar therefore grow more and more tensile

Figure 2: Thermal strain ($\mu\epsilon$), joint design A

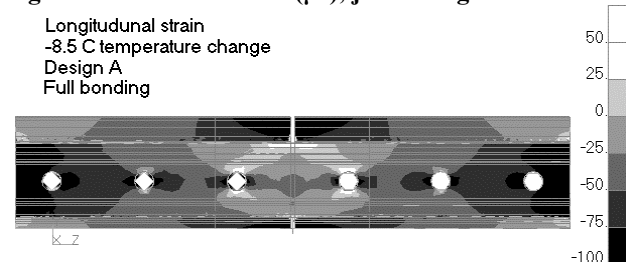
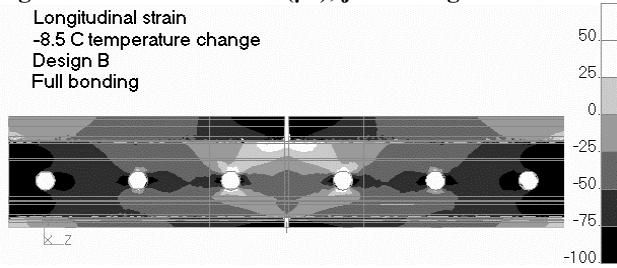


Figure 3: Thermal strain ($\mu\epsilon$), joint design B



towards the center, as the epoxy layer transfers the tension from the rails to the bars. At the endpost, all of the tension has been transferred, and the rail ends are free to contract to their natural size. The outside surface of the joint bar near the endpost experiences a total strain of up to about $+25 \mu\epsilon$ – implying that a tensile strain of $+125 \mu\epsilon$ was imposed on top of the natural contraction.

It is interesting to note that the tensile forces actually cause negative bending in the joint bars, causing the endpost to deflect upwards by a small amount. This implies that the neutral axis of the rails is slightly above the neutral axis of the bars, so that the contraction of the rails causes an eccentric loading in the bars. This is relevant because it implies that strains will be more tensile at the top of the joint bar and more compressive at the bottom.

As the epoxy bond degrades at the center of the joint, the tensile forces must be transferred from rail to bar over a shorter distance. At the endpost, where no force is being transferred, the strains in the joint bar tend to equalize along the length of the unbonded region. That force is transferred closer to the ends of the joint bar, making the strains there more tensile. This is evident in Figures 4 and 5, which show the same joint design and the same

Figure 4: Thermal strain ($\mu\epsilon$), design A, 90 mm debonding

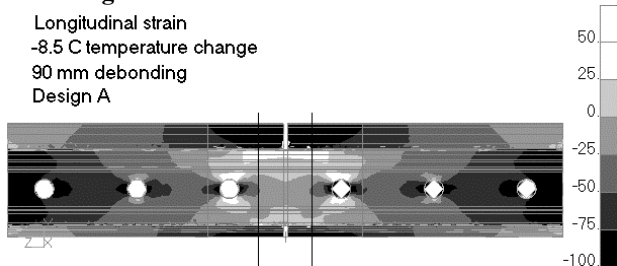
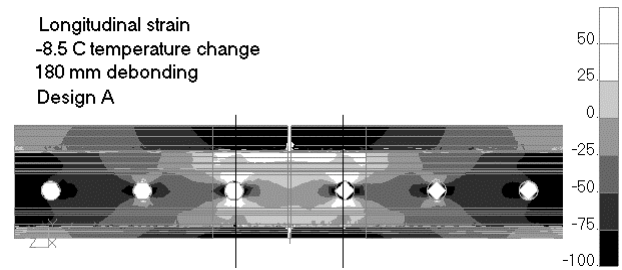


Figure 5: Thermal strain ($\mu\epsilon$), design A, 180 mm debonding



loadings as in Figure 2, but with an increasingly large area of epoxy debonding. The black lines indicate the boundaries of the debonded area.

Note that stress also changes across the joint bar section, as shown in Figure 6. As the epoxy debonds, stresses near the center of the debonded area become more evenly distributed in the lateral direction, taking the distribution shown in Figure 7. The somewhat surprising effect is that debonding can actually increase the strain on the outside surface of the joint bar near the endpost, as can be seen in Figures 2 and 5.

To determine the actual shape of a debonded area requires destructive disassembly of the joint. Such testing has shown that the debonded area typically has a shape that is roughly rectangular, at least in the critical areas

nearest the endpost. The bond on one joint bar may degrade faster than on the other joint bar. According to our analysis, this leads to bending in the transverse direction, increases the strain in the joint bar with more debonding and decreases it in the other joint bar. An example of the results is shown in

Figure 6: Strain ($\mu\epsilon$) in joint bar

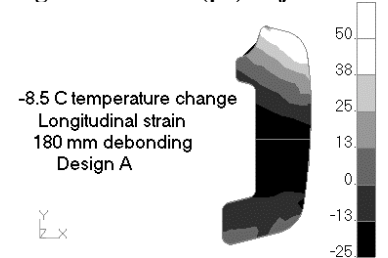


Figure 7: Strain ($\mu\epsilon$) in joint bar, 180 mm debonding

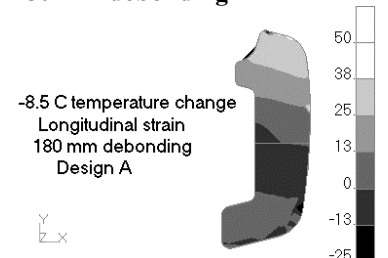


Figure 8, which shows strain in a joint with 89 mm (3.5 in.) of debonding on one side and 140 mm (5.5 in.) on the second.

We suggest that, for a fully bonded joint, the joint bar strain decreases from the center of the joint bar, except for localized effects caused by the bolt holes. As the epoxy bond deteriorates, the gradient of the strain near the endpost decreases, leaving the strain at the center of the joint bar more uniform. As a consequence, the ratio of the strain near the center of the joint bar and the strain at a point farther away from the center decreases as the debonded area expands.

5. LABORATORY TESTING

In order to study the mechanical effects of joint deterioration, we are conducting a test program at the University of Illinois Newmark Structural Engineering Laboratory. Tensile loads are applied to a series of insulated joints specimens. These specimens include a control group, consisting of two new, previously unused joints, and a test group of joints that have been removed from track due to unspecified service failures.

5.1 Test goals and methods

The test setup consists of a horizontally mounted hydraulic actuator mounted on a reaction block; the insulated joint plug is bolted (through the rail's neutral axis) to the actuator piston. The other end

Figure 8: Thermal strain ($\mu\epsilon$), asymmetric debonding

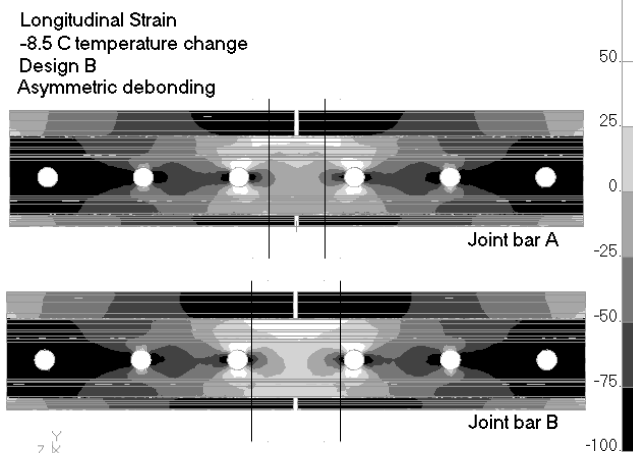
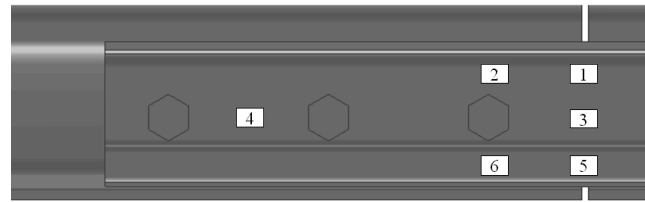


Figure 9: Strain gauge locations



of the joint plug is bolted to another reaction block. Because the testing is intended to simulate thermally induced loads, loading is applied slowly, not exceeding 10 kN/s (2 kip/s). The actuator is rated for loads of up to 445 kN (100 kips); problems with the fixtures have so far limited the actual applied loads to 178 kN (40 kips). Conventional foil strain gauges applied to various parts of the joint bars allow us to measure the actual strain distribution within the joint. The approximate positions of these strain gauges are shown in Figure 9. The pattern shown in the figure is for one half of one of the two joint bars and is repeated on zero to three of the other half joint bars, depending on the specimen. Other strain gauges placed on the rail a short distance away from the joint measure the actual input forces, to correct for unintentional shear or bending.

Our objective is to compare the control specimens to the failed specimens in order to find the effects of epoxy debonding. However, because the samples use a mixture of several different rail weights and joint bar designs, such comparisons cannot be done directly. Instead, the control specimens must be used to verify and refine the finite element model; then, this verified model can be used to generate predictions about the behavior of debonded joints, which are verified and refined through tests on the failed joints.

The goal of this iterative process is to determine where a set of smart strain gauges should be mounted in order to track epoxy debonding. The controlled laboratory environment is different from the situation in the field, where loads are less predictable and variation between installations is quite likely. Therefore, the promising sensor locations identified in the lab are used only as guidance for a later phase of field testing.

5.2 Laboratory analysis

Tests to date include one control specimen (with joint bar design B) and one failed specimen (with joint bar design A). If both joints were fully bonded, we would predict strains equal to the tensile portion of the combined contraction / tension pattern seen in Figure 2 for the control and Figure 3 for the failed joint. In other words, adding back the 100 $\mu\epsilon$ of stress-neutral thermal strain to the strain distribution shown in the figures gives us the predicted strains under laboratory tensile loads.

Table 1

Experimental strains for control joint

Gauge	Measured $\mu\epsilon$	Predicted $\mu\epsilon$
1	131	116
2	67	76
3	52	51
4	32	29
5	50	48
6	45	50

Table 1 compares the predicted and measured strains at various locations on the joint bar for the control specimen. Only one half of one joint bar was instrumented completely, on the assumption that a joint with fully bonding on both bars would be symmetric.

Table 2

Experimental strain ratios for control joint

Gauge1 / Gauge2	Measured ratio	Predicted ratio
1/2	1.96	1.53
3/4	1.64	1.84
5/6	1.11	0.96

Table 2 shows the predicted and measured values of the *ratios* of strains for strain gauges at the same height (gauges 1 and 2, 3 and 4, and 5 and 6). The general trend of higher surface strains at the endpost, decreasing towards the end of the bar, is confirmed by the experiment. However, the strains measured near the center of the joint bar are lower

than predicted, while the strains measured near the end of the bar are somewhat higher than predicted.

Table 3 shows some of the results from the test on a failed joint with visible signs of epoxy debonding. The extent of the visible damage on the top edge of the epoxy stretched away from the endpost for 230 mm (9 in.) to the right and 210 mm (8.25 in.) to the left on one joint bar, and 140 mm (5.5 in.) to the right and 280 mm (11 in.) to the left on the other. On each joint bar, the visually evident debonding on the bottom edge of the epoxy layer was more limited, extending for no more than about 75 mm (3 in.).

Table 3

Experimental strain measurements for failed joint

Gauge	Measured $\mu\epsilon$	Predicted $\mu\epsilon$ (fully bonded)	Predicted $\mu\epsilon$ (debonding model)
1A	102	84	102
2A	107	89	115
3A	82	66	87
4A	39	33	34
1B	130	83	123
2B	134	87	110
3B	97	63	98
4B	41	33	35

For this test, sensors were applied to both joint bars; the joint bar location is as shown in Figure 9, with an A or B to indicate the joint bar. The measured values were compared to several different models: one for a fully-bonded joint of this design (Figure 2), and others representing various possible areas of epoxy debonding. No model exactly predicted the measured strains. The closest match came from including 89 mm (3.5 in) of debonding on joint bar A and 140 mm (5.5 in) on joint bar B, the pattern shown in Figure 8. This debonding model predicts two important trends: higher strain on one joint bar than the other (from the uneven bonding), and increased stress at the exterior joint bar surface as suggested by Figures 6 and 7.

6. SENSOR NETWORK DESIGN

With some idea of how strain changes in a debonding joint, we can turn our attention to how to measure the strain in the field using smart sensors. The design of the sensor network itself is incomplete, but some principles are understood.

Smart strain gauges all have on-board, low-power radios that can automatically form mesh networks using the ZigBee networking protocol. Maximum range for these radios is estimated at around 50 to 90 meters (150 to 300 feet). The radio dominates the electrical power requirements of the device. Fortunately, ZigBee networks by design can have extremely low radio duty cycles. Processing the data using the onboard processor and transmitting only summary statistics also minimizes the amount of data that must be sent over the radio.

With the expected radio duty cycle, the sensors should be able to run off a small battery for weeks or months. In order to meet actual operational requirements, the sensors would additionally need some way to harvest energy from the environment, such as by trickle charging from the track circuit.

To be useful, the results obtained by the sensor network must be passed on to railroad personnel. This is accomplished via a gateway of some kind, for instance, an interface to a more powerful IEEE 802.11 (Wi-Fi) network that could be accessed from a moving vehicle. Such an interface would need to be connected to an external source of power, and therefore would be located away from the tracks but within the range of the ZigBee radio – for instance, in the signal cabinet that stands near many mainline insulated joints.

7. CONCLUSIONS

Preliminary results show that the measurable strains in bonded insulated joints in response to longitudinal loads correlate with the presence of epoxy debonding. This change could be tracked by a system of smart strain gauges, providing more in-

formation about joint health while requiring minimal human attention.

Ongoing research will develop specific failure signatures that the sensors can use to determine autonomously when a joint requires attention. Field testing will be needed to ensure that these signatures are identifiable in real-world situations.

ACKNOWLEDGEMENTS

Research funded by the Association of American Railroads. We are grateful to David Davis and Mohammad Akhtar, Transportation Technology Center, Inc.; Norfolk Southern (especially the Illinois Division); CN; Portec Rail Products; and LB Foster Co. The first author was supported in part by a CN Railroad Engineering Research Fellowship.

REFERENCES

- [1] Kerr, Arnold D. and Cox, Joel E. "Analysis and tests of bonded insulated rail joints subjected to vertical wheel loads," *International Journal of Mechanical Sciences*, v 41, n10, Oct, 1999, p 1253-1272.
- [2] Davis, David D. et al. "Effects of heavy axle loads on bonded insulated joint performance," *Proceedings of the 2005 American Railway and Engineering Association Annual Conference*, 2005.
- [3] *United States Code of Federal Regulations*, Title 49, Section 213.119.g.
- [4] See "Home Heartbeat" product, Eaton Electrical, Inc. <http://www.homeheartbeat.com>
- [5] <http://www.zigbee.com>
- [6] Hay, William W. *Railroad Engineering*, 2nd ed., John Wiley and Sons, New York: 1982, p 548-550.
- [7] Kerr, Arnold. *Fundamentals of Railway Track Engineering*, Simmons-Boardman Books, Omaha: 2003